

Modeling Flow Features with User-Guided Streamline Parameterization

Luoting Fu^a Levent Burak Kara^{a,*} Kenji Shimada^a

^aDepartment of Mechanical Engineering, Carnegie Mellon University, 5000 Forbes Ave, Pittsburgh, PA 15213, USA

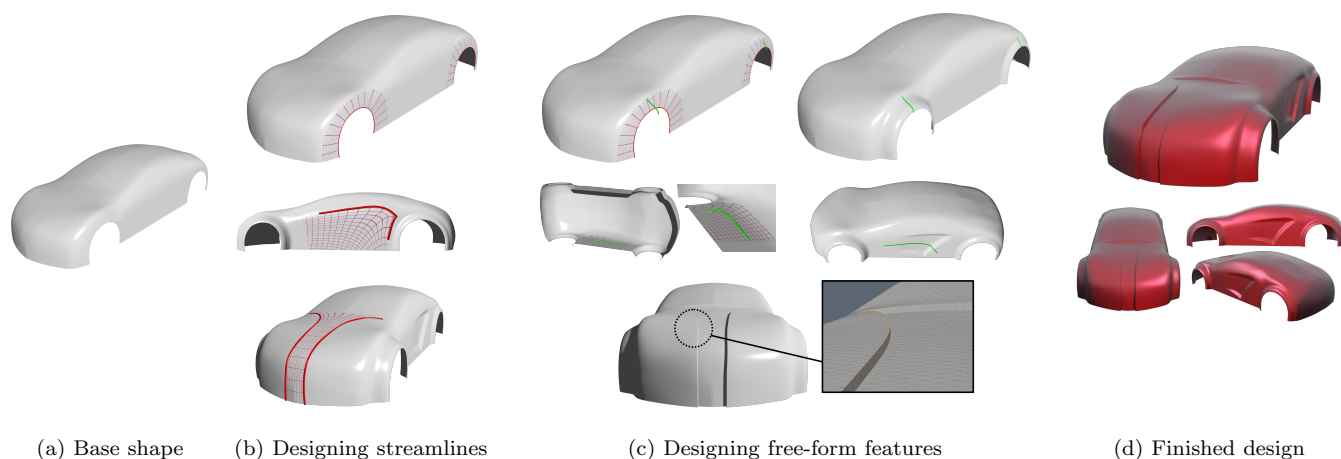


Fig. 1. Overview of a typical session using the described system. In column (b), the designer first draws streamline constraints (red strokes) on the surface to generate a singularity-free parameterization (red and blue grids). Then the designer draws shape editing strokes (green) to drive displacement maps and create free-form features (column c). The cuts on the hood (3rd row of column c) was created via a downward extrusion.

Abstract

Streamline-like, free-form features that “flow” on a base shape are often utilized in the design of products ranging from automobiles to everyday consumer products. Providing computational support for the design of such features is challenging, because of the open-endedness of the design explorations involved, and the necessity to rapidly and precisely capture the design intents expressed in very simple forms, such as free-form sketches. We present a novel approach for designing streamline-based, free-form surface features in the context of product design. Using our approach, the user first designs a network of streamlines on the base shape, by performing a stroke-constrained mesh parameterization. Then, the user utilizes these streamlines as a curvilinear scaffold for creating 3D free-form features that are bounded and parameterized by these streamlines. The user is able to apply fine-grained control of the outline, profile and extent of the resulting 3D features by manipulating the streamlines. We demonstrate the capability of this approach on several product models.

Key words: constrained mesh parameterization, vector field, sketch-based modeling, streamline, displacement mapping

1. Introduction

Many shape features in product design can be abstracted as streamline-like features that “flow” on the base shapes. This abstraction encompasses a wide range of geometric

features, such as creases, channels, ridges, bulges, which bear critical implications on the aesthetic and ergonomic aspects of the product [9,16]. They are prevalent in various media and stages in conceptual design. Examples include those shown in Figure 2.

Developing aesthetically pleasing, streamline-like surface features on product forms has been a long standing chal-

* lkara@cmu.edu. Address correspondence to this author.

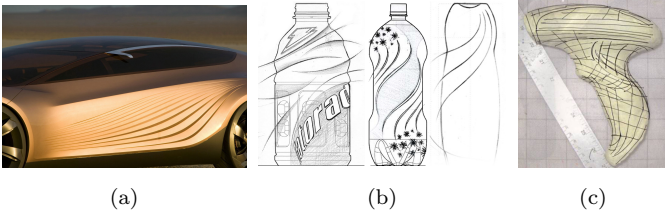


Fig. 2. Streamline-based features in conceptual design. (a) A photorealistic rendering of the streamline features on the side panel of Mazda Nagare. (b) Packaging design sketches by Christopher Lavelanet utilizing streamlines. (c) An informal streamline sketch made as an overlay on a clay model by DiMonte Group.

12 lence in industrial design. Designers approach this chal-
 13 lenge by strategically prototyping and evaluating many
 14 shape design alternatives, especially in the early conceptual
 15 stages [14]. Computational design tools should support the
 16 rapid creation and exploration of such shape features. How-
 17 ever, the existing free-form modeling systems, such as para-
 18 metric surface modeling tools, subdivision modeling tools
 19 and mesh sculpting tools, do not cater to such needs. With
 20 those tools, the designer will have to rely on indirect and
 21 incremental editing metaphors such as parametric control
 22 points, or mesh sculpting tools and engage in tedious trial-
 23 and-error of shape editing workflow, or distractive work-
 24 flows such as UV editing and re-topology.

25 We provide an approach for streamline-based, free-form
 26 modeling that enables direct prescription of the desired
 27 streamline patterns and shape profiles, the rapid explo-
 28 ration and the fine-grained user control of the resulting
 29 shapes.

30 1.1. Overview of User Interaction

31 Our approach is built on “streamlines”. Mathematically,
 32 the streamlines refer to the isolines in the (u, v) parame-
 33 terization, visualized using a red-blue grid texture. Prac-
 34 tically, the streamlines are the geometric scaffold for con-
 35 structing free-form, 3D features that are aligned, bounded
 36 and parameterized by them.

37 In a typical editing scenario shown in Figure 1, our sys-
 38 tem works on a 2-manifold, triangular mesh \mathcal{M} , and alter-
 39 nates between two modes: surface streamline design (Fig-
 40 ure 1b) and 3D feature editing (Figure 1c). Both modes are
 41 driven by the input strokes drawn by the user.

42 In the streamline design mode, the user controls the
 43 shape of the flow by drawing constraint strokes. The sys-
 44 tem will populate two sets of isolines over the user-selected
 45 region of interest on the base shape. One set, the stream-
 46 lines, will interpolate the constraint strokes, and vary in
 47 between the constraints. The other set, the equipotential
 48 set, will be approximately orthogonal to the streamlines.
 49 The details are described in Section 3.

50 In the 3D feature design mode, the user utilizes these
 51 streamlines as a curved scaffold to sketch and build 3D free-
 52 form features. The user specifies the extremity and profile
 53 of the resulting features by drawing outline strokes along

54 the streamlines, and drawing cross-section strokes across
 55 the streamlines, respectively. The system deforms the base
 56 surface with a displacement map $d(u, v)$ parameterized by
 57 the streamlines (u, v) , such that the created feature inter-
 58 polates the strokes. The details are presented in Section 4.

59 Our technical contributions include the construction of
 60 smooth surface editing handles through the interactive pre-
 61 scription of characteristic streamlines, a linearized tech-
 62 nique for fine-tuning the alignment of the field-guided pa-
 63 rameterization, and a streamline-based curvilinear scaffold
 64 for unprojecting shape editing sketches and driving 3D free-
 65 form feature creation.

66 2. Related Work

67 The construction of on-surface streamlines pertains to
 68 mesh parameterization. Research in surface mesh param-
 69 eterization has generated a large body of literature. For a
 70 review of the progress in this field, we refer to several sur-
 71 vey papers [6,15,3,1].

Our method is built on field-guided mesh parameteri-
 zation. This family of methods aims to compute a global,
 piece-wise linear parameterization from a guidance vector
 field pre-computed for each triangle t in the mesh \mathcal{M} . Math-
 ematically, the unknowns to be solved are the (u, v) coor-
 dinates for each vertex, and they are the minimizers for the
 variational problem

$$\min_{u,v} \sum_{t \in \mathcal{M}} (\|\tau_t - \nabla u_t\|^2 + \|J\tau_t - \nabla v_t\|^2) w_t, \quad (1)$$

72 where ∇ is the face-wise gradient operator [3], τ_t is a tangent
 73 guidance vector usually computed to follow the principal
 74 curvature directions, $J\tau_t$ is the rotation of τ_t by $\pi/2$, and
 75 w_t is a weighting factor proportional to the area of face t . u_t
 76 and v_t represent the u, v coordinates of vertices belonging
 77 to face t on the mesh.

78 This is a well studied objective function [12,7,2,10,1]. It
 79 minimizes the misalignment between the gradient direc-
 80 tions of u, v and the guidance vector. However, the objec-
 81 tive alone is insufficient to generate isolines aligned with
 82 the constraint strokes: the isometry of the objective tends
 83 to create uniformly spaced isoline grids, and deviate the
 84 isolines away from the constraints. Several remedies have
 85 been proposed to break isometry and improve alignment
 86 with the constraints, though at the cost of computation ef-
 87 ficiency [8,10], linearization assumption [12], user interven-
 88 tion [2], or reduced user interaction such as processing a
 89 single stroke only [13].

90 3. Streamline Design by User-Guided 91 Parameterization

92 Streamline design is the first step of our shape editing
 93 workflow. As illustrated in Figure 1b, this step does not
 94 entail any shape modification, but generates the geometric
 95 scaffold that supports subsequent editing. We compute the

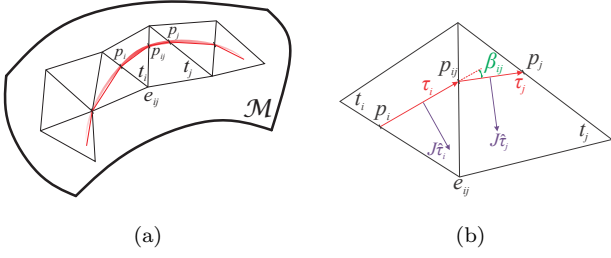


Fig. 3. The generation and use of streamlines per the user’s constraint strokes. (a) A triangle strip in \mathcal{M} constrained by a streamline stroke (red). (b) Two adjacent triangles t_i and t_j in the constrained strip of faces.

96 streamlines by a constrained, field-guided mesh parameterization described below. The variables to be determined
 97 are the (u, v) parameters for each vertex in \mathcal{M} . To produce
 98 streamlines suitable for aesthetic design, we seek to align
 99 streamlines maximally to the user-drawn constraints, and
 100 avoid singularities such as sinks, sources or vortex centers.
 101

102 3.1. Vector Field Design

103 In Figure 3a, we first sample the user constraint strokes as
 104 polylines, and project them onto \mathcal{M} to find the intersections
 105 with the edges. In Figure 3b, the constraints computed
 106 include the tangent direction τ of the segment contained
 107 within each face, and the intersection p .

108 We then follow the approach of trivial connections [5], a
 109 particularly efficient and robust method, to compute a discrete, face-wise, tangent vector field $\tau_t, t \in \mathcal{M}$ per the directional constraints. For each face within a disc-like region selected by the user, we compute a directional vector via constrained linear least squares to ensure that the resulting field varies minimally and smoothly. To avoid singularities, we insert a phantom vertex connected to all the boundary vertices of the disc region, to form a topological sphere. We then assign a singularity index of 2 to the phantom vertex to concentrate the unavoidable singularity away from the surface, because the Poincaré-Hopf Theorem maintains that the total singularity of a vector field on the sphere is 2. See Figure 6 for an example of the constraints and the resulting vector field.
 120
 121
 122

123 3.2. Constrained Parameterization with Fine-Tuning

Our goal here is to compute a piece-wise linear parameterization from the guidance vector field. The unknowns are the (u, v) coordinates of each vertex, and are computed by

$$\min_{u,v} \sum_{t \in \mathcal{M}} (\|s_t \tau_t - \nabla u_t\|^2 + \|s_t J \tau_t - \nabla v_t\|^2) w_t \quad (2)$$

s.t. $u_i = u_j, \forall p_i, p_j \in$ the same constraint stroke.

124 The notation is similar to the parameterization objective
 125 (Equation 1) reviewed in Section 2. Here we have made the

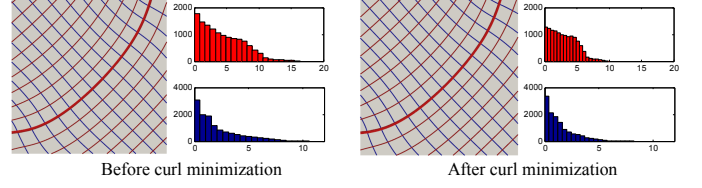


Fig. 4. The effect of curl-minimization on parameterization. The test case is the parameterization of a quad domain with one constraint (bold red strokes). The histograms show the angular mismatches between the direction of the parameterization and the guidance vector field. The red and blue histograms represent the mismatch for the u and v parameters, respectively.

following two additions to this equation to adapt to our application scenario. 126 127

Firstly, we have added a face-wise scaling factor s_t to scale the length of each guidance vector, to reduce the curl of the field which is non-integrable and causes a residual misalignment between the smooth vector field and the parameterization. The discrete curl [11] of τ at each shared edge e_{ij} in Figure 3b is

$$\text{curl}(\tau)_{e_{ij}} = -\tau_i \cdot e_{ij} + \tau_j \cdot e_{ij}, \quad (3)$$

which suggests that by scaling τ_i per the ratio of its projection onto e_{ij} and that of τ_j , the curl at e_{ij} will be canceled locally. Globally, however, we can only hope to minimize, rather than completely cancel, the total curl of the vector field. To do so, we model the scaling factor s_{ij} on edge e_{ij} such that

$$\min_{s_{ij}} \sum_{i,j \in \mathcal{M}} \|s_{ij} - \frac{\tau_i \cdot e_{ij}}{\tau_j \cdot e_{ij}}\|^2 \quad (4)$$

s.t. $\prod_j s_{ij} = 1, \forall$ vertices j adjacent to vertex i .

The product constraint ensures the global consistency of the scaling factors, such that any path between two faces will accumulate the same amount of scaling. We solve for $\log s_{ij}$ instead of s_{ij} to obtain a linear system, that is

$$\min_{s_{ij}} \sum_{e \in \mathcal{M}} \|\log s_{ij} - \log(\frac{\tau_i \cdot e_{ij}}{\tau_j \cdot e_{ij}})\|^2 \quad (5)$$

s.t. $\sum_j \log s_{ij} = 0, \forall$ vertices j adjacent to vertex i .

After solving for the edge-wise scaling factors s_{ij} , we recover the face-wise scaling factor s_t by traversing the mesh, and multiplying the scaling factors when crossing an edge. Figure 4 shows the effect of curl minimization on reducing the directional mismatch between the parameterization and the guidance vector field.
 128
 129
 130
 131
 132
 133

The vector field computed may contain curl irremovable by scaling, and solving Equation 5 may result in large scaling factors. We therefore restrict the scaling factors to $[\frac{1}{5}, 5]$ which is the typical range of the gradient magnitudes for a number of smooth parameterization that we reverse-engineered. Additionally, the user can choose to fall back to an un-scaled version where $s_t = 1, t \in \mathcal{M}$.
 134
 135
 136
 137
 138
 139

Secondly, we add the equality constraints to explicitly enforce the alignment between the streamlines and the constraint strokes. For instance, in Figure 3b, the intersections between the mesh edges and the constraint stroke, namely
 140
 141
 142
 143
 144

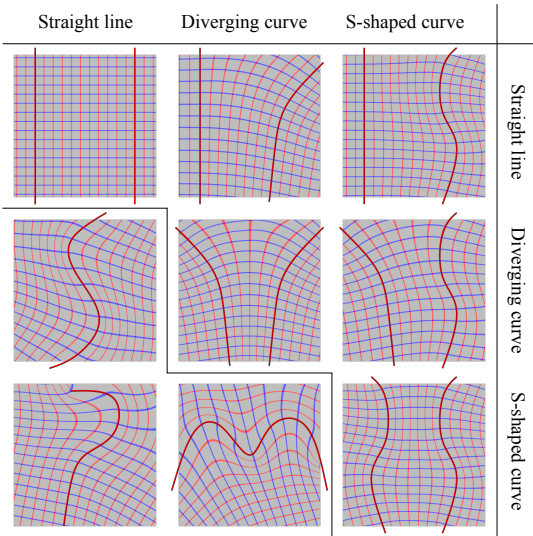


Fig. 5. A matrix view of streamline parameterizations generated on a plane with various constraints. In the upper triangle of the 3 matrix, we apply the row constraints on the left, and the column constraints on the right. Due to the symmetry of the constraints, we only show the combinations in the upper triangle, and use the space in the lower triangle to stress-test the parameterization method with highly curved, irregular constraints. The narrow, red and blue lines are the streamlines. The brighter, red lines are the constraint strokes drawn by the user.

points p_i , p_j and p_{ij} , are constrained to the equal u coordinates. This requires expressing the value u_i of edge point p_i in terms of the u of the vertices, and trivially translates into a linear, barycentric interpolation.

3.3. Evaluations

Figure 5 shows several synthetic examples of the streamlines generated with different combinations of constraints. In all cases, the streamlines interpolate the constraint strokes up to numerical precision. Figure 6 shows several examples of streamlines created on the curved surface of a shampoo bottle.

We summarize the total time taken from the constraint processing to completion of the parameterization on several models in Table 1, and the results compare favorably with the reported performance of existing works such as conjugate direction field [10], but not on par with the single stroke parameterization of [13]. This performance difference represents a trade-off between functionality (handling multiple constraint strokes) *versus* simplicity (handling one input constraint stroke).

4. Shape Editing using Streamlines

4.1. Curved Scaffold for Sketch-based Shape Modeling

First, we use the streamlines on the surface as a curved scaffold, and perform the stroke unprojection with their aid, as illustrated in Figure 7. We first unproject the end points

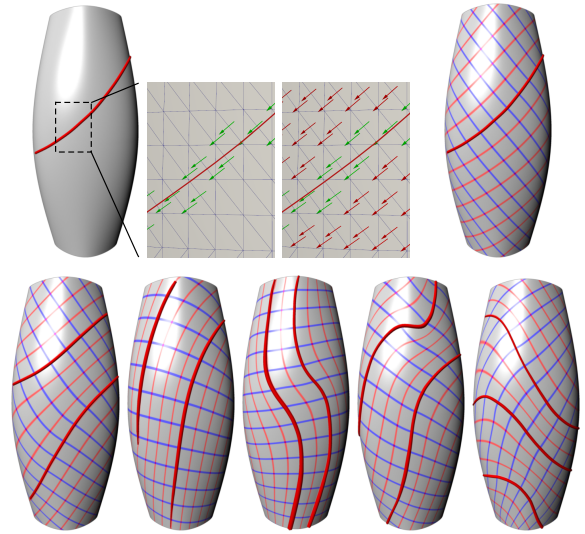


Fig. 6. Curved streamlines generated on a curved base surface. The narrow red and blue lines are the streamlines. The wide red lines are the constraint strokes drawn by the user. The first row also shows the handling of the user constraints and the guidance vector field. The green arrows are the face-wise directional constraints computed from the constraint stroke, and the red arrows represent the guidance vector field computed from the directional constraints.

Table 1

Run-time statistics on benchmark models. Run-times are measured in seconds on a 2.6GHz Intel quad core CPU with 16GB of RAM, the same as that of [10]. The hardware of [13] is unclear. Our solver utilizes multi-cores. The timing of [10] is based on the reported values. The timing of [13] is interpolated from the performance curve from their Figure 13. For models tested in [10], we selected ones that are homomorphic to a disc. See the Figure 6 of [10] for the models.

Model	#Tri	Our Method	Baselines
Tower	6751	0.17	5.4 [10], ≈ 0.01 [13]
Shell	7214	0.14	0.91 [10], ≈ 0.01 [13]
Roof	10979	0.28	23.4 [10] ≈ 0.02 [13]
Bottle	8192	0.21	≈ 0.01 [13]
Car	6786	0.15	≈ 0.01 [13]
Mouse	20000	0.51	≈ 0.04 [13]

of the editing stroke to the surface, and select the closest streamline as the *source* curve. We then extrude each point s_i on the source curve along a user-customizable direction n_i , and create a quad strip. This quad strip serves as a curved scaffold, upon which we project the entire editing stroke, and resolve their 3D locations in the model space. We label the resulting 3D points the *target* t_i . Finally, we compute $t - s$, the local displacement induced by the editing stroke, which we will propagate throughout the region of interest in Section 4.2.

4.2. Procedural Displacement Mapping

In this step, the local edits induced by the editing stroke ($t - s$) are propagated globally along the streamlines, in

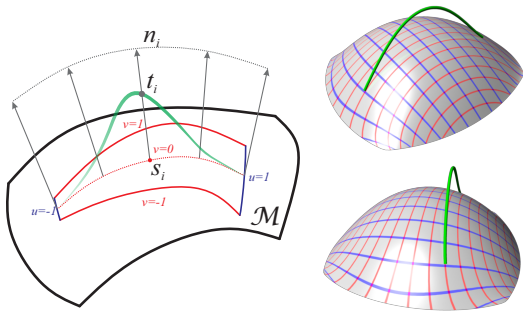


Fig. 7. Streamlines (red and blue) as a curved scaffold for inferring the 3D location of a shape editing stroke (green). Top right: The stroke drawn in the screen space. Bottom right: The stroke unprojected parallel to the viewing plane, and then viewed from a different view.

the form of a procedural displacement map. During the propagation, the magnitude of the displacement vector is adjusted per a *fall-off* function which controls the cross-section profile of the resulting free-form feature. Unlike the existing sketch-based modeling systems that base the fall-offs on the geodesic distance on the surface, or a global energy functional [4], we compute the fall-off in the (u, v) space spanned by the streamlines. The resulting features will flow along the user-designed streamlines, rather than following intrinsic geometric traces such as the lines of curvature or geodesics. The displacement scalar d of a vertex with parameters (u, v) is determined by

$$d(u, v) = d_u(u)d_v(v), \forall u \in [-1, 1], v \in [-1, 1], \quad (6)$$

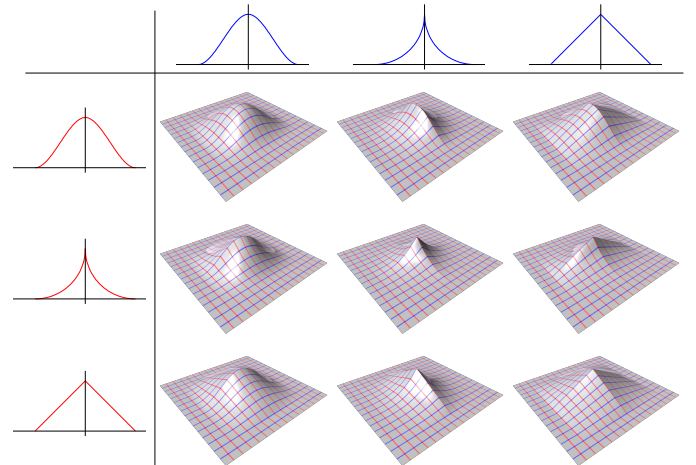
181 such that two 1D fall-off functions d_u and d_v , adjustable by
 182 the user, jointly controls the displacement.

183 Figure 8 showcases a variety of free-form features gener-
 184 ated using our approach. By allowing various combinations
 185 of streamline patterns and displacement maps, we provide
 186 the user with flexibility in various design scenarios.

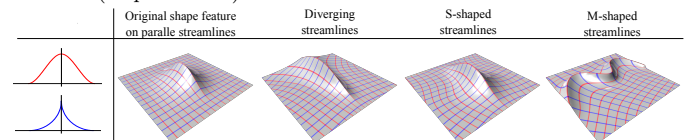
187 Displacement map is not the only surface editing tech-
 188 nique compatible with the streamlines. Any deformation
 189 approach that relies on a pair of source and target curves to
 190 drive the deformation is suitable. We choose displacement
 191 map here due to its closed form and efficiency.

192 5. Design Examples

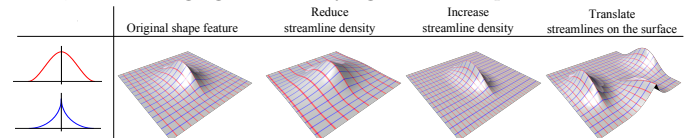
193 We showcase several design examples with complex free-
 194 form features created from minimal user inputs. Figure
 195 9b shows our system utilized in the design of an asym-
 196 metric mouse, which features a number of smooth and
 197 semi-smooth creases that flow through the shape. Figure
 198 9a shows our system utilized for the design exploration of
 199 shampoo bottles. Our system follows the conventional, pen-
 200 and-paper design work-flow that has led to the 2D design
 201 sketches in the first column, and extends the design into the
 202 3D space. Finally, we showcase another car design session
 203 in Figure 10.



(a) Different shape features generated by keeping the streamline patterns constant, while varying the shape profiles (*i.e.*, displacement fall-offs) along the red, blue streamlines. For each shape, the profiles along the red (resp. blue) streamlines are the functions plotted in the row (resp. column) header in the same color.



(b) Different shape features generated by keeping the fall-offs constant, while changing the underlying streamline patterns.



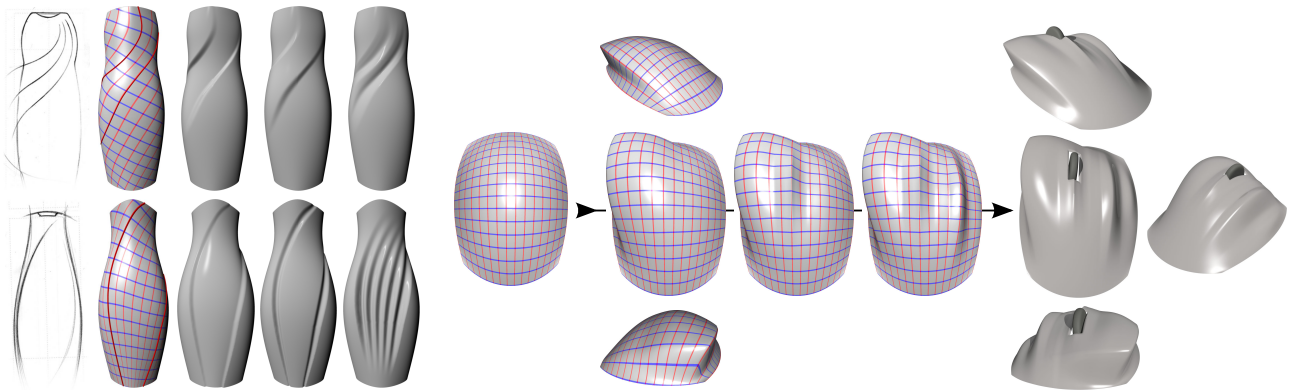
(c) Different shape features generated by keeping the fall-offs and streamline patterns constant, while transforming the streamlines by scaling or translating the (u, v) coordinates of the vertices. In the last column we display three instances of uv -translated shape features, two of which are partially out of the domain boundary. We note that this show our displacement-based scheme is not limited to local bump-like features, but also open channels extending out of the surface boundary.

Fig. 8. Shape feature variations created with a combination of different fall-off functions and streamline patterns.

204 6. Concluding Remarks

205 We have developed a novel, streamline-based shape edit-
 206 ing system intended for streamline-like features that flow
 207 on a base shape, such as creases, ridges, and valleys. It has
 208 several advantages, including the ease of use, fine-grained
 209 user control of the outline, profile and extent of the result-
 210 ing features, and the capability to explore the shape design
 211 space along such dimensions. Our design case studies have
 212 initially demonstrated the potential of this method.

213 Current limitations of our system include the lack of sup-
 214 port for designing streamline fields with intended singular-
 215 ities such as sources and vortices, and artifacts when work-
 216 ing with a low-density input mesh.



(a) Shampoo bottles design starting from concept sketches (first column).

(b) The design of a feature-rich, asymmetric mouse. The middle row shows the evolution of the design. The top and bottom row provide alternative perspectives.

Fig. 9. Design examples.

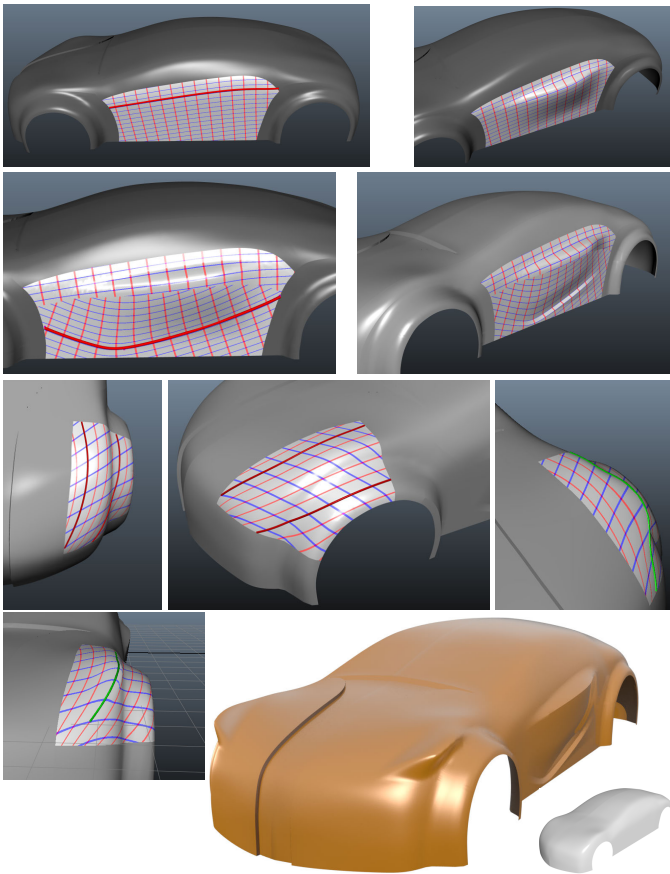


Fig. 10. A car design session. Streamlines are drawn as the red and blue curves on the surface. The streamline editing strokes are rendered as the bold, red strokes. The shape editing strokes are rendered as the green strokes. The starting shape is shown in the bottom right corner.

217 References

218 [1] David Bommes, Bruno Levy, Nico Pietroni, Enrico Puppo,
219 Claudio Silva, Marco Tarini, and Denis Zorin. Quad-mesh
220 generation and processing: A survey. *Computer Graphics Forum*,
221 In Press:no-no, 2013.
222 [2] David Bommes, Henrik Zimmer, and Leif Kobbelt. Mixed-
223 integer quadrangulation. In *ACM SIGGRAPH 2009 papers*,

SIGGRAPH '09, pages 77:1–77:10, New York, NY, USA, 2009. 224
ACM. 225
[3] Mario Botsch, Leif Kobbelt, Mark Pauly, Pierre Alliez, and 226
Bruno Levy. *Polygon Mesh Processing*. AK Peters, 2010. 227
[4] Mario Botsch and Olga Sorkine. On linear variational surface 228
deformation methods. *IEEE Transactions on Visualization and*
Computer Graphics, 14(1):213–230, January 2008. 229
[5] Keenan Crane, Mathieu Desbrun, and Peter Schroder. Trivial 231
connections on discrete surfaces. *Computer Graphics Forum*,
29(5):1525–1533, 2010. 232
[6] MichaelS. Floater and Kai Hormann. Surface parameterization: 234
a tutorial and survey. In NeilA. Dodgson, MichaelS. Floater,
and MalcolmA. Sabin, editors, *Advances in Multiresolution for*
Geometric Modelling, Mathematics and Visualization, pages 235
157–186. Springer Berlin Heidelberg, 2005. 236
[7] Felix Kalberer, Matthias Nieser, and Konrad Polthier. 237
Quadcover - surface parameterization using branched coverings. 238
Computer Graphics Forum, 26(3):375–384, 2007. 239
[8] Denis Kovacs, Ashish Myles, and Denis Zorin. Anisotropic 240
quadrangulation. In *Proceedings of the 14th ACM Symposium*
on Solid and Physical Modeling, SPM '10, pages 137–146, New 241
York, NY, USA, 2010. ACM. 242
[9] Tony Lewin and Ryan Borroff. *How to Design Cars like a Pro*. 243
MBI Publishing, 2010. 244
[10] Yang Liu, Weiwei Xu, Jun Wang, Lifeng Zhu, Baining Guo, 245
Falai Chen, and Guoping Wang. General planar quadrilateral 246
mesh design using conjugate direction field. *ACM Trans. Graph.*,
30(6):140:1–140:10, December 2011. 247
[11] Konrad Polthier and Eike Preuss. Identifying vector field 248
singularities using a discrete hodge decomposition. In 249
Visualization and Mathematics III, pages 113–134. Springer 250
Verlag, 2003. 251
[12] Nicolas Ray, Wan Chiu Li, Bruno Lévy, Alla Sheffer, and Pierre 252
Alliez. Periodic global parameterization. *ACM Trans. Graph.*,
25(4):1460–1485, October 2006. 253
[13] Ryan Schmidt. Stroke parameterization. *EUROGRAPHICS* 254
Computer Graphics Forum., In Press:8, 2013. 255
[14] J. J. Shah. Collaborative sketching (c-sketch) - an idea 256
generation technique for engineering design. *Journal of Creative*
Behavior, 35(3), 2001. 257
[15] Alla Sheffer, Emil Praun, and Kenneth Rose. Mesh 258
parameterization methods and their applications. *Foundations*
and Trends in Computer Graphics and Vision, 2(2):105–171,
January 2006. 259
[16] Roselien Steur and Koos Eissen. *Sketching: drawing techniques* 260
for product designers. BIS Publishers, Netherland, 2009. 261
262
263
264
265
266
267
268
269